Iron limitation – A perspective on a growth-restricted cultivation strategy for a H_2 production system using the diazotrophic cyanobacterium *Nostoc* PCC 7120 *ΔhupW*

Christoph Howe[a], Daniel Becker[b], Christian Steinweg[b], Clemens Posten[b], Karin Stensjö[a,*]

[a] *Department of Chemistry-Ångström Laboratory, Uppsala University, 75120 Uppsala, Sweden*
[b] *Karlsruhe Institute of Technology (KIT), Institute of Process Engineering in Life Sciences III Bioprocess Engineering, 76131 Karlsruhe, Germany*

ARTICLE INFO

ABSTRACT

H_2 is a promising carbon-free alternative to fossil fuels, and can be photoautotrophically produced by cyanobacteria. Despite efforts to increase cyanobacterial H_2 production by genetic engineering and technical optimization the yield remains economically non-viable. Recent studies have therefore demanded the impairment of growth to reallocate more carbohydrates into biofuel biosynthesis, and nutrient limitation may be a strategy to achieve that. Here we show that limitation of Fe in the filamentous and heterocystous mutant strain *Nostoc* PCC 7120 *ΔhupW* resulted in a 5.3-fold lower chlorophyll *a* concentration as compared to the controls during four-week cultivation. The Fe-limited filaments contained a heterocyst frequency at ~6% and a 4-fold higher specific carbohydrate concentration as compared to the control cultures. We discuss whether Fe-limiting conditions leading to an accumulation of carbon storage compounds could be used as a heterocyst based H_2 production system.

1. Introduction

In the past decades, cyanobacteria have gained growing interest to be used for renewable hydrogen production based on sunlight, water and a small amount of nutrients (Nagarajan et al., 2017). Especially diazotrophic and filamentous cyanobacteria have been intensively studied as a chassis for H_2 production. These bacteria mainly possess photosynthetic vegetative cells but under conditions of N-deprivation they can develop heterocysts, a specialized cell type for N_2-fixation. Heterocysts are a key element in photobiological hydrogen production as H_2 is a byproduct of the N_2 reduction reaction to NH_3 (Khetkorn et al., 2013). It is the microoxic environment inside the heterocysts that allows the O_2-sensitive nitrogenase to function. The electrons for the N_2 reduction are originally gained from photosynthetically produced carbohydrates in the vegetative cells. These sugars are transported into the heterocysts and catabolized in concert by the oxidative pentose phosphate pathway, glycolysis, respiration and cyclic photosynthesis to feed the nitrogenase with the necessary ATP and electrons (Magnuson, 2019). Due to the spatially separated processes of photosynthesis and hydrogen formation that requires the formation of carbohydrates, the process is referred to as indirect photolysis (Prince and Kheshgi, 2005).

Due to the poor H_2 yields in the past 30 years of research, many

strategies have been followed to enhance the cyanobacterial H_2 production, summarized in numerous reviews (Khetkorn et al., 2013; Saifuddin and Priatharsini, 2016; Sakurai et al., 2015). Some of these strategies required genetic modifications such as the truncation of antenna complexes for more efficient light distribution across the culture (Liberton et al., 2013), increasing the heterocyst frequencies (Masukawa et al., 2017) as well as re-designing of the nitrogenase enzyme (Masukawa et al., 2010). In the broader field of cyanobacterial biosynthesis research a key strategy has been the restriction of the glycogen synthesis/storage to reallocate the carbon source for cellular growth and biosynthesis (Luan et al., 2019). While most of these attempts resulted in impaired cyanobacterial growth accompanied with reduced cellular fitness, a successfully increased biofuel synthesis was achieved only in some cases but still far from being economically viable. However, also technical parameters during cyanobacterial cultivation have been optimized to enhance H_2 production. Several studies have shown that changes in the chemical composition of the culture medium, light intensity, gas phase, pH or temperature can enhance H_2 production (Ananyev et al., 2008; Berberoğlu et al., 2008; Yeager et al., 2011). Even though knowledge about optimal growth conditions, often similarly interpreted as optimal hydrogen production conditions, was gained, a breakthrough in H_2 production yields was not reached: During

---

the past 30 years, the highest energetic photon-to-H_2 conversion peak efficiencies of indirect photolysis utilizing the nitrogenase-driven process reached ~4% (Nyberg et al., 2015), far from its theoretical maximum of 16.3% assuming photons of 680 nm (Prince and Kheshgi, 2005). During outdoor experiments, efficiencies close to 0.2% display the usual maximum after a few days of cultivation (Sakurai et al., 2015). Summarizing the generally poor results of cyanobacterial biosynthesis research it was hypothesized that there might be a critical distinction between optimal conditions for growth and enhanced biofuel production (Rodionova et al., 2017). Even more recently it was concluded that attempts to arrest biomass accumulation could be a key element to enhance the efficiency of bio-compound synthesis (Luan et al., 2019). Therefore, it may not be a question about how much product can be gained from a growing cyanobacterial culture, but how much energy, which is naturally reserved for growth, can be allocated towards biofuel production. To date, little is known about cyanobacterial cultivation processes that aim to limit growth in regards to the aspects of biofuel production.

Arresting cyanobacterial growth can be achieved in different ways. Besides genetic engineering, nutrient limitation displays a potent approach as there are many essential nutrients in the metabolism of cyanobacteria (Quigg, 2016). One of them is iron. The importance of Fe has been widely studied in cyanobacteria (Straus, 1994) as it is incorporated as a co-factor in hemes and iron sulphur clusters for electron transfer processes such as photosynthesis, respiration and N_2-fixation (Straus, 1994; Kranzler et al., 2013). Iron starvation has been reported to frequently occur in nature (Boyd et al., 2007) and the physiological effects of iron limitation have been explored for a series of cyanobacteria e.g. *Trichodesmium erythraeum*, *Calothrix parietina*, *Synechococcus* sp. strain PCC 7942 and *Nostoc* PCC 7120 (Narayan et al., 2011; Shi et al., 2007; Yingping et al., 2014). Generally, cyanobacteria can adapt to iron deprivation by three major processes. One of them is cellular retrenchment including the degradation of phycobilisomes as suggested for *Synechococcus elongatus* PCC 7942 and PCC 7002 (Hardie et al., 1983; Sherman and Sherman, 1983). Phycobilisomes are pigment protein complexes that serve as an antenna for light capturing and their biosynthesis relies on Fe-containing enzymes (Straus, 1994). The second major effect of iron starvation is exchanging iron–demanding enzymes such as ferredoxins with the iron-free counterparts for example flavodoxins (Narayan et al., 2011). As a third major adaptation to iron starvation, some cyanobacteria enhance their capacity for iron acquisition by e.g. the excretion of iron-binding siderophores (Kranzler et al., 2013). It appears that different cyanobacterial clades react differently to iron limitation. In non-diazotrophic cyanobacteria, iron limitation has been observed to lead to the effects of chlorosis, which have been suggested to be due to a co-limitation of nitrogen (Hardie et al., 1983; Sherman and Sherman, 1983). On the other hand, diazotrophic cyanobacteria showed decreased growth rates and an increased accumulation of carbon-based storage compounds such as polyglucoside granules or glycogen (Jacq et al., 2014; Sherman and Sherman, 1983; Shi et al., 2007; van Alphen et al., 2018). However, the effects of Fe limitation in diazotrophic and filamentous cyanobacteria have not been discussed in connection to biohydrogen formation. For the purpose of biofuel production in general, only rare examples exist which try to utilize the effects of nutrient limitation combining it with genetic modification (Melis et al., 2000).

One of the model species for the investigation of H_2 production via indirect photolysis is *Nostoc* PCC 7120 Δ*hupW*, a filamentous and heterocystous cyanobacterium. This strain lacks a functional uptake hydrogenase that re-oxidize the H_2 produced by nitrogenase enzyme complex (Lindberg et al., 2012; Nyberg et al., 2015). As a result, the produced H_2 immediately leaves the heterocysts.

This study aims to explore whether iron limitation could be used as a cultivation strategy for H_2 production in *Nostoc* PCC 7120 Δ*hupW*. As a main focus we were interested whether the amount of heterocysts would be maintained throughout a cultivation time of four weeks, as

heterocysts display a key element to the process of H_2 production. We monitored the optical density and chlorophyll concentration of the cultures to analyze the effects of iron starvation on growth limitation and determined the carbohydrate concentration at the end of the cultivation as carbohydrate storage could display a key role in transforming photosynthetic energy into H_2.

2. Materials and methods

2.1. Strains and growth conditions

All experiments were performed using a Δ*hupW* strain of the filamentous heterocystous cyanobacterium *Nostoc* PCC 7120 (Lindberg et al., 2012). The gene *hupW* encodes the specific protease responsible for the last maturation step of the uptake hydrogenase (HupSL protein). Therefore *Nostoc* PCC 7120 Δ*hupW* does not comprise a functional uptake hydrogenase and H_2, produced by the nitrogenase, will not be consumed but released from the cells. It should be noted that this cyanobacterial mutant strain still possesses a bidirectional hydrogenase encoded by the *hox* gene that has not been shown to contribute to H_2 production (Masukawa et al., 2002). Cell cultivation was performed under sterile conditions in a final volume of 215 mL suspension cultures in modified nitrogen-deprived $BG11_0$ medium (N_2 fixing-conditions) (Rippka et al., 1979) without EDTA. EDTA is a potent chelator agent for Fe^{3+} (Brausam et al., 2009) and it could interfere with the undertaken ion chromatography analysis during the study. To study the effect of Fe starvation, the Fe salts were exchanged to Na salts in the $BG11_0\Delta EDTA\Delta Fe^{3+}$ medium. The pH of the culture media was set to 7.5 by the addition of 9 mM HEPES buffer and 4.5 mM $NaHCO_3$ and did not change during the experiment (data not shown). All cultivation was performed at 25 °C under temperature control, 100 rpm continuous agitation and aerobic conditions. The cultures were illuminated with 20 μmol $m^{-2} s^{-1}$ for 12 h between 6:00 AM – 18:00 PM via LED panels, while otherwise kept in darkness. The initial OD_{800nm} in all experiments was 0.05. The inoculum originated from a culture cultivated in $BG11_0\Delta EDTA$ medium and the estimated Fe concentration in the Fe-limited culture was approximately reduced by 43-fold as compared to standard $BG11_0$. Digital images of the cultures were documented with the camera Samsung ST77.

2.2. Chlorophyll a determination and optical density of cells

For the quantification of the chlorophyll *a* concentration (Chl a), 500 μL samples were collected from each culture and treated as described in a methanol-based extraction protocol (Zavřel et al., 2015). The standard deviation was calculated based on three biological replicates with two technical replicates. For centrifugation the MIKRO 220R centrifuge (Hettich) was used. Growth curves were obtained by plotting the measured optical density at 800 nm (OD_{800nm}) against time and the standard deviation was calculated from three biological replicates with two technical replicates. For spectroscopic analyses the UV/Vis spectrophotometer Lambda 35 (PerkinElmer) was utilized run by the UV WinLab software (PerkinElmer).

2.3. Microscopy and estimation of heterocyst frequency

To determine the heterocyst frequency, each culture was microscopically investigated using a light microscope (Axio Scope A1 HAL 100, Carl Zeiss Microscopy GmbH) with a 40× objective in differential interference contrast mode (DIC). From each of the three biological replicates, a total number of > 1000 cells (both vegetative cells and heterocysts) were counted based on microscope images (Salleh et al., 2016). Images at a total magnification of 400× were documented by using the digital camera INFINITY2-3C (Lumenera Corporation) and the software INFINITY ANALYZE 2 (Lumenera Corporation). Microscopic images from the cultures over the entire cultivation time can be

accessed from the web deposit: http://dx.doi.org/10.17632/hs8kkr6mgg.1. The heterocyst frequency was expressed as a percentage of the total number of cells. The error bars of the heterocyst frequency represent the standard deviation of three biological replicates. Multiple heterocysts located adjacent to each other in the same filament were counted as a single heterocyst. Proheterocysts were taken into account for counting, whereas heterocysts that were not integrated within a filament were not counted (Salleh et al., 2016).

2.4. Carbohydrate quantification

To determine the carbohydrate concentration a colorimetric approach was chosen (Yemm and Willis, 1954). For this, 1 mL samples of a culture were centrifuged (MIKRO 220R centrifuge, Hettich) for 7 min at 15,000 ×g at 4 °C. The supernatant was discarded and the cell pellets were stored at −20 °C. After resuspending with dH$_2$O, 400 μL sample volume was added to 800 μL 0.1% (*w/v*) anthrone in 95% H$_2$SO$_4$. After mixing, the samples were kept on ice for 5 min. Thereafter, the samples were incubated in a thermoincubator at 95 °C at 300 rpm for 16 min and then kept on ice for 5 min. The absorbance at 625 nm was measured with the UV/Vis spectrophotometer Lambda 35 (PerkinElmer) run by the UV WinLab software (PerkinElmer) at which the reaction product between furfural and anthrone has its absorbance maximum (Yemm and Willis, 1954). For carbohydrate quantification, a dilution series of a starch standard was prepared ranging from 0 to 0.075 g/L (Zulkowsky GR for analysis, MERCK). The standard deviation was calculated based on three biological replicates with two technical replicates. The specific carbohydrate concentration reflects the total carbohydrate concentration normalized on the chlorophyll *a* concentration.

2.5. H$_2$ quantification

For H$_2$ production analysis, specially designed Erlenmeyer flasks were used that comprised a thread to close with PTFE O-ring and plastic screw caps with apertures (Duran Group) (Fig. 1). The total volume of the Erlenmeyer flask was about 400 mL and at a filling of a 215 mL culture the headspace volume was 185 mL. Between the PTFE O-ring and plastic lid a stainless steel metal plate with two openings was inserted. One opening, defined as the inlet, was connected to a mass flow controller (MKS) unit to provide air at a flow rate of 4.5 mL min^{-1}. All mass flow controllers were calibrated using a low flow cell gilibrator (Gilian). The second opening of the Erlenmeyer flask, defined as the outlet, was connected to the gas chromatograph unit 3000A Micro GC (Agilent Technologies) run with the software EZChrome SI (Agilent Technologies). The column Molsieve (10 m × 320 μm × 12 μm) served for gas separation and was set to 110 °C at a pressure of 30 psi. Argon (99.999%, Air Liquide Deutschland GmbH) was used as a carrier gas in the GC. Gas injection (10 ms) into the inlet volume kept at 80 °C was performed every ~3 min and the gas was analyzed by a thermal conductivity detector (TCD). Multiple cultures were analyzed by a self-built automated gas switch system. When switching to the next cultivation vessel, the GC was supplied with the exhaust gas of the analyzed cultivation vessel for 20 min before quantitative data on the gas mixture was recorded. The whole setup (Fig. 1) was designed in order to acquire quantitative H$_2$ production data without the risk of overpressure or internal gas-circulation enriching O$_2$ in the gas phase that has been reported to negatively affect nitrogenase activity (Staal et al., 2001). The LED panel and mass flow controllers were controlled via the software LabView. Data from the GC was redirected automatically to LabView to collect time-resolved H$_2$ production. For quantitative H$_2$ analysis the following standard gases were utilized: 100 ppm H$_2$ in air (Calgaz), 200 ppm H$_2$ in air (Calgaz), 5% H$_2$ (Air Liquide) and 50% H$_2$ (Air Liquide). We verified the setup of H$_2$ quantification on cultures of *Nostoc* PCC 7120 Δ*hupW* strain by switching the gas input from air to argon. This resulted in an approximately four-fold increase in H$_2$ production under standard Fe condition which is in accordance with earlier results (Nyberg et al., 2015).

2.6. Inductively coupled plasma optical emission spectroscopy ICP-OES

The elemental analysis (Mn, Mg, P, K, Ca, Fe, Co and Mo) of the cyanobacterial cultures was conducted via inductively coupled plasma optical emission spectroscopy (ICP-OES) using an iCAP 7600 Duo (Thermo Scientific). To separate the elements in the soluble phase from the insoluble phase, a volume of 148.5 mL was taken from the standard culture medium as well as from cell cultures grown for 28 days under the control condition and centrifuged at 4000 rpm for 40 min at 25 °C. For the soluble phase, 7.5 mL of the supernatant was sampled, whereas for the insoluble phase, a volume of 7.5 mL containing the complete pellet was collected. Each sample of 7.5 mL was solubilized by adding 10 mL HCl (sub boiled grade), 1 mL HNO$_3$ (sub boiled grade), 1 mL hydrogen peroxide (suprapur, Merck) and 0.5 mL hydrogen fluoride (suprapur, Merck) and heated in a microwave oven (speedwave Xpert, Berghof). After the solubilization, the volume of the samples were set to 50 mL and diluted to proper concentrations for the ICP-OES measurement. Dependent on the element, two or three major wavelengths of the elemental emission spectra were used for quantification. The analysis of the components was accomplished with four different calibration solutions with the internal standard scandium. The range of the calibration solutions did not exceed a decade and included values received from the samples. The calibration was verified by the use of further calibration solution from other manufacturers and charges. The quantification for all the elements was within the detection limit. The culture medium evaporation which was measured to be approximately 310 μL per day during the cultivation of 28 days was considered for

A

B
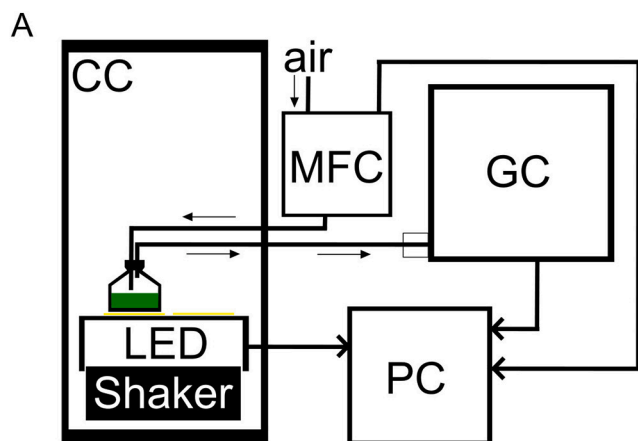
Fig. 1. Scheme of the on-line setup for the detection of H$_2$ production from a culture of *Nostoc* PCC 7120 Δ*hupW*. The personal computer (PC) was connected to the LED panel, gas chromatograph (GC) and mass flow controllers (MFC). The MFC, connected to a source of air, provided a constant air flow at 4.5 mL min^{-1} into the cultivation vessel. The exhaust gas mixture was directed to the GC for quantitative gas analysis. The shaker and the cultivation chamber (CC), kept at 25 °C, were autonomous machines. B Image of a cultivation vessel containing 210 mL medium prepared for GC measurement.
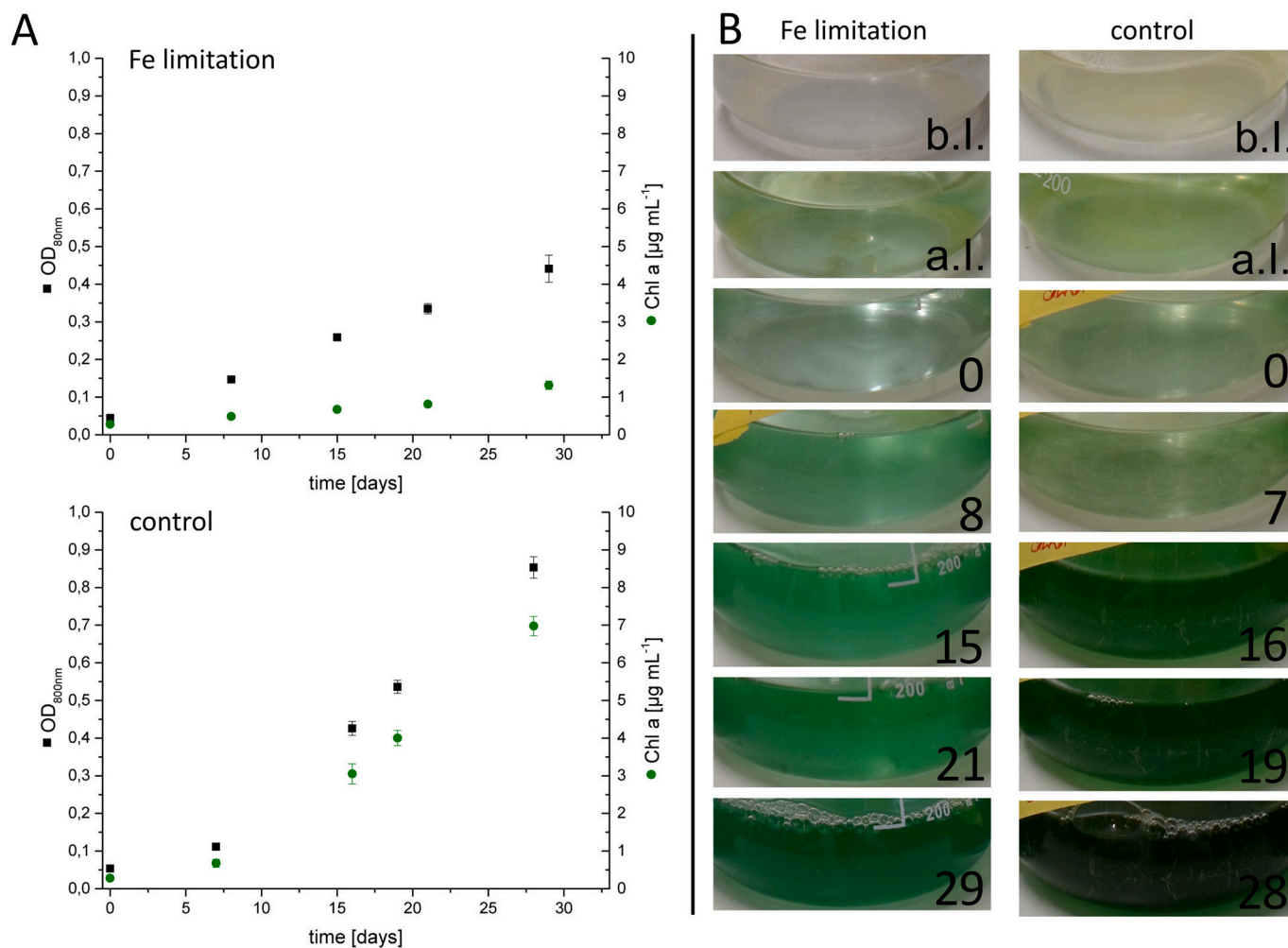
Fig. 2. Reduced growth of *Nostoc* PCC 7120 Δ*hupW* under Fe limited conditions. A Growth curves and the chlorophyll *a* concentration of the *Nostoc* PCC 7120 Δ*hupW* in diazotrophic conditions under Fe limitation. Optical density at 800 nm (OD$_{800nm}$, black squares) and chlorophyll a concentration (Chl a, green circles) in µg mL^{-1} plotted against the cultivation time. Cultivation performed under Fe-limited and control condition. All cultures were grown at 20 µmol photons m^{-2} s^{-1} (12 h light/ 12 h darkness), 100 rpm agitation at 25 °C for approximately four weeks. Each data point represents a biological triplicate with technical duplicates and error bars indicate the standard deviation. B Culture images of Fe limited and control cultures of *Nostoc* PCC 7120 Δ*hupW*. The documentation day during the cultivation is indicated in each picture. An image of the respective culture medium before inoculation (b.I.) is given. All cultures were grown at 20 µmol photons m^{-2} s^{-1} (12 h light/12 h darkness), 100 rpm agitation at 25 °C for approximately four weeks.

calculations. Cu and Zn contaminations from the pipes in the water source were verified and did not allow further quantification.

3. Results and discussion

### 3.1. Fe-limitation restricts growth in Nostoc PCC 7120 ΔhupW

To evaluate to what extent Fe limitation affects the growth of the cyanobacterium *Nostoc* PCC 7120 Δ*hupW*, quantitative spectroscopic methods were used to determine the optical density at 800 nm (OD$_{800nm}$) and the chlorophyll *a* concentration of the living cells during cultivation. A long cultivation period (four weeks) was chosen to evaluate whether the nutrient limitation could be utilized in the purpose of future H$_2$ production (Fig. 2). Long term cultivation processes are useful to test for phenotypical changes of the cells and for the viability of the culture. A quantitative elemental analysis on the control cultures after the cultivation period ensured that, among various elements, macronutrients such as phosphor, potassium and magnesium were still abundant in the culture medium, hence elemental co-limitation under Fe-limiting conditions could be excluded (Table 1).

The cultures of *Nostoc* PCC 7120 Δ*hupW* under Fe limitation grew

Table 1

Elemental quantification of cyanobacterial uptake from the control culture medium. Mass difference of the supernatant/pellet based on elements found in the supernatant/pellet of the cyanobacterial culture after 28 days of cultivation subtracted by those quantified in the supernatant of the culture medium. All mass changes refer to a sample volume of 148.5 mL. Based on the given mass differences a molar and normalized elemental ratio of the cyanobacterial elemental uptake stoichiometry was estimated:Mn$_{1.0}$Mg$_{63}$P$_{112}$K$_{80}$Ca$_{27}$Fe$_{6.3-10}$Co$_{0.039}$Mo$_{0.058-0.11}$.

Element	Mass difference [mg] supernatant	Mass difference [mg] pellet	Elemental mass ratio of cell pellet to total element amount [%]
Mg	−0.1527	0.1679	14.2
P	−0.3644	0.3792	44.4
K	−0.3255	0.3423	15.8
Ca	−0.0996	0.1161	7.41
Mn	−0.0052	0.0060	7.93
Fe	−0.0385	0.0632	31.7
Co	−0.0002	0.0003	11.7
Mo	−0.0006	0.0011	4.73
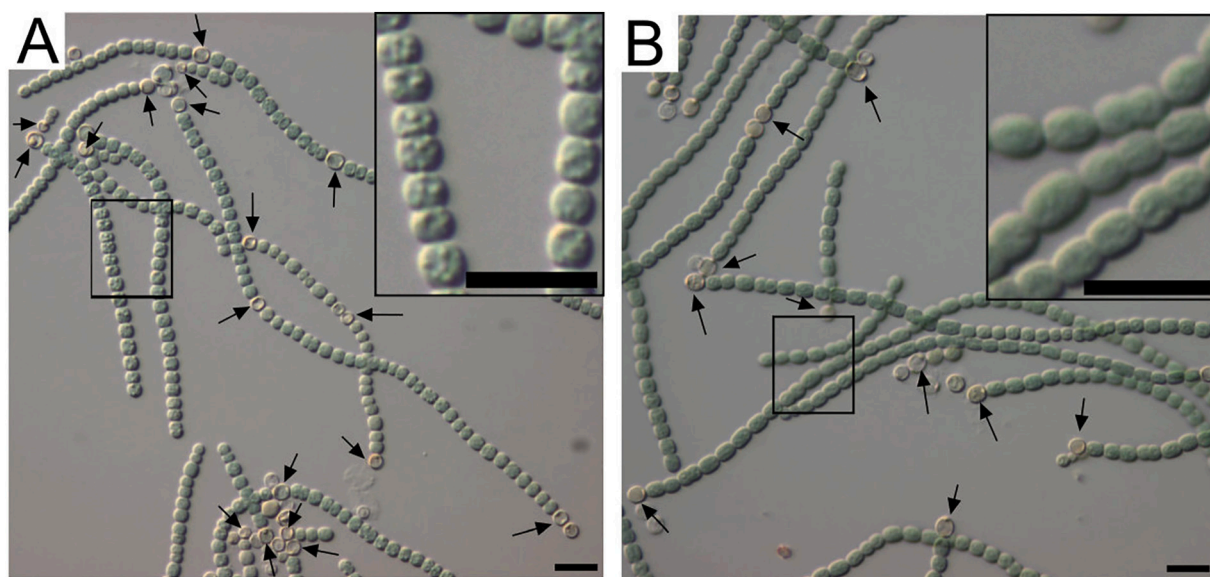
Fig. 3. The limitation of Fe led to an accumulation of storage compounds. Microscopic images of A. Fe-limited culture on day 21 and B. control culture on day 28. Image magnifications give insights on the accumulation of cellular storage compounds under iron limitation compared to the control conditions. All black bars represent a length of 10 μm and arrows indicate heterocysts that are integrated inside the filaments.

about five times slower as compared to the control cultures as determined by total chlorophyll *a* accumulation (Fig. 2A). Despite this growth retardation, the Fe-limited cells were viable over the entire cultivation period of four weeks under the tested condition (Fig. 2B). The OD_{800nm} and the Chl a concentration of the cultures under the Fe-limited condition linearly increased from $0.045 \pm 0,001$ to 0.44 ± 0.04 and from 0.28 ± 0.01 μg mL^{-1} to 1.3 ± 0.1 μg mL^{-1}, respectively, over the four weeks of cultivation time (Fig. 2A). No halted state of growth was found under Fe-limitation. The control culture also showed a linear increase of the OD_{800nm} and Chl a concentration but resulting in higher final values of 0.85 ± 0.03 and 7.0 ± 0.3 μg mL^{-1}, respectively (Fig. 2A). In agreement with our observation, it has been previously shown that wildtype cultures of *Nostoc* PCC 7120 proliferate for 90 days under iron starvation (Narayan et al., 2011). It should be noted that the Fe-limited samples reached a ~1.9 fold lower OD_{800nm} by the end of the experiment as compared to the control samples, but their Chl a concentration was ~5.3 fold lower. Under standard growth condition a similar rate of increase for OD_{800nm} and Chl is expected, but under Fe limited conditions *Nostoc* PCC 7120 Δ*hupW* showed a reduction in cell size by approximately 30% (Fig. 3). A similar observation was reported for the cyanobacterium *Synechocystis* sp. PCC 6803 upon iron starvation (Schoffman and Keren, 2019).

3.2. Under Fe limitation Nostoc PCC 7120 ΔhupW accumulates higher levels of carbohydrate storage compounds than the control culture

Monitoring the optical density and the Chl a concentration gave insights on the growth of the cultures under iron limitation but it did not provide information on other cellular parameters that could potentially affect the H_2 production capacities, such as the filament length, heterocyst frequency as well as the accumulation of storage compounds. The microscopic analyses revealed that under Fe-limited conditions, the filaments were long and contained heterocysts during the four week experiment, similar to the control samples (Fig. 3). Furthermore, it was observed that many vegetative cells in the Fe-limited filaments were partially filled with round particles with diameters up to 1 μm (Fig. 3A). These particles are most likely storage compounds such as glycogen storage. Glycogen is a branching polymer of glucose and is commonly observed in cyanobacteria (Luan et al., 2019).

To investigate whether the observed storage compounds are chemically based on carbohydrates such as glycogen, a quantitative analysis of the total amount of cellular carbohydrates at the end of the four week cultivation was performed. The Fe-limited samples contained 1.8 mg carb $μg^{-1}$ Chl a $^{-1}$, while the control samples contained 0.46 mg carb $μg^{-1}$ Chl a $^{-1}$ culture. This 4-fold higher specific carbohydrate concentration supported the microscopic observation of more and larger storage compounds. An accumulation of carbohydrate storage compounds has been observed for iron-deprived filamentous cyanobacteria (Sherman and Sherman, 1983; Shi et al., 2007; van Alphen et al., 2018) and is an indication for an active photosynthetic machinery and CO_2-fixation. In indirect photolysis processes, photosynthetically active carbon fixation is desired as the chemical energy of the accumulated carbohydrates is aimed to be subjected to H_2 producing enzymes inside the heterocysts. However, a study on *Nostoc* PCC 7120 showed a ~50% lower PSII activity and C-uptake under Fe-limitations as compared to control conditions in a 90 days experiment (Narayan et al., 2011). Iron limitation may downregulate the photosynthetic activity and CO_2-fixation, but these effects could be due the general limitation of growth.

The introduction of heterologously expressed enzymes to reallocate accumulated carbon compounds may overcome these negative effects. Additionally, genetic engineering of *Nostoc* PCC 7120 Δ*hupW*, e.g. by the introduction of effective photo-fermentative pathways inside heterocysts (Kars and Gündüz, 2010), such as the insertion of a H_2-producing hydrogenase, might allow for restored photosynthetic activity and CO_2-fixation.

3.3. The heterocysts of the Fe-limited Nostoc PCC 7120 ΔhupW as a chassis for H₂ production

The heterocyst frequency is an important factor for H_2 production since heterocysts display the chassis for H_2 production (Masukawa et al., 2017). The heterocyst frequency must be retained throughout the nutrient limitation phase, thus the detachment of these heterocysts from the filament is undesired (Salleh et al., 2016).

In this study, microscopic images of the Fe-limited cultures were used to estimate the heterocyst frequency of the filaments during the four weeks cultivation while comparing to control conditions. The microscopic analysis showed that the Fe-limited cultures possessed a
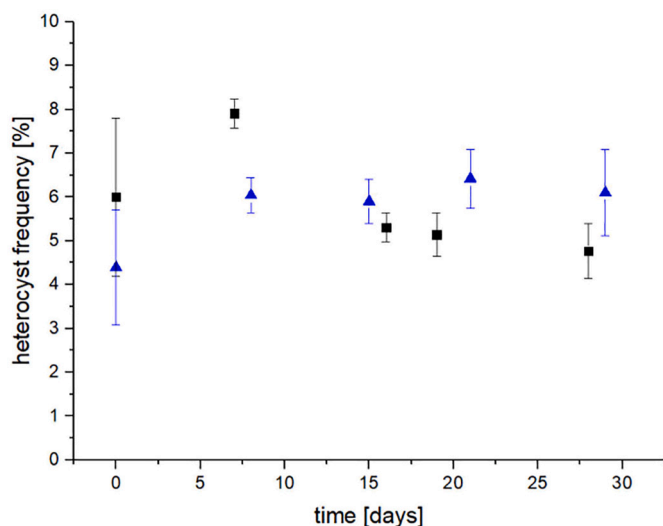
Fig. 4. Heterocyst frequency (%) of filaments under Fe-limited and control conditions. The heterocyst frequency in the Fe-limited (blue triangles) and control cultures (black squares). Except of day zero, all data points represent > 3000 counted cells (vegetative cells and heterocysts) from three biological replicates (count of > 1000 per replicate) and the error bars indicate the standard deviation. For data points on day zero > 1000 cells were counted from the inoculation culture that was grown under similar conditions as the control and the standard deviation was set to 30%, the highest experimentally observed one.

similar frequency of heterocysts throughout the entire experiment (Fig. 4). The initial heterocyst frequency was ~4.4% on day zero for the Fe-limited cultures. The cultures possessed heterocyst frequencies ranging between ~5.9% - 6.4% during the four subsequent weeks of the experiment. The control cultures contained higher heterocyst frequencies of 6% and 7.9% on day zero as well as on day seven respectively. On the other hand the heterocyst frequency in the control cultures decreased to approximately 4.8% towards the end of the experiment between day 16 and 28 (Fig. 4).

Similar to our observations for *Nostoc* PCC 7120 Δ*hupW*, also the diazotrophic cyanobacterium *Calothrix parietina* possessed an increased heterocyst frequency under iron starvation as compared to control conditions (Dougals et al., 1986). In general, data on heterocyst frequency during nutrient-limiting conditions is rare. It remains unclear why heterocysts are retained under Fe-limiting conditions for a prolonged time period. To what extent the heterocyst-rich cellular state and the carbohydrate accumulation under Fe limitation is affected by external parameters such as light intensity and temperature needs to be investigated, as both light and temperature are key factors defining the optimal conditions in future outdoor H_2 production systems (Rodionova et al., 2017). Utilizing the micro-oxic environment inside heterocysts enables O_2-sensitive enzymes such as hydrogenases and nitrogenase to function. Hydrogenases generally possess substantially higher turnover frequencies, have no ATP requirements and they have higher photon-to-H_2 conversion efficiencies, as compared to nitrogenases (Khetkorn et al., 2013). Nitrogenase-catalyzed H_2 production is less efficient comparing to hydrogenases (Nagarajan et al., 2017), and hydrogenases have been recognized as the more potent hydrogen producing enzymes (Nagarajan et al., 2017). In this study, nitrogenase-derived H_2 of Fe-limited cultures of *Nostoc* PCC 7120 Δ*hupW* was below the detection limit from day seven and onwards during the cultivation (data not shown). Based on the growth retardation under Fe limitation, a reduced productivity of H_2 was expected as the N_2 fixation process it is tightly linked to growth. For the control cultures an exponentially decreasing H_2 productivity, normalized to Chl a concentration, was observed throughout the experiment (Fig. 5). Similar findings have been reported earlier (Borodin et al., 2000; Lindblad et al., 2002) and might be linked
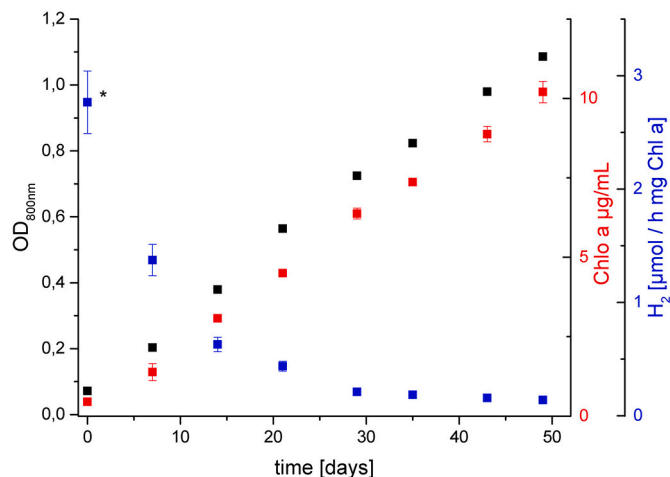
Fig. 5. H_2 productivity and growth of *Nostoc* PCC 7120 Δ*hupW* under control conditions. The graph depicts the OD_{800nm} (black squares), the Chl a concentration (red squares) and the peak H_2 production rate, normalized on the total Chl a content of the culture (blue squares). Peak production was visible for about 6 h of the 12 h illumination period each day. The culture was grown at 20 μmol photons m^{-1} s^{-1} (12 h light/12 h darkness), 100 rpm agitation at 25 °C. *Chl a amount measured on day 0 was used to calculate H_2 production rate on day 1.

to a decreasing light intensity per cell during continuous growth (Liberton et al., 2013). But how could a non-growth-driven H_2 production be implemented in the Fe-limited cells?

One of the most prominent goals in the field of biohydrogen research is the introduction of a H_2-producing [FeFe] hydrogenase into the heterocysts of filamentous diazotrophic cyanobacteria to increase H_2 production yields (Avilan et al., 2018). Even though the introduction of a [FeFe] hydrogenase has been reported in *Nostoc* PCC 7120, higher levels of H_2 production have not been achieved yet. If successfully introduced to heterocysts of Fe-limited filaments, the [FeFe] hydrogenase would require iron during the Fe limited cultivation. The Fe requirements of [FeFe] hydrogenases are similar as for other hydrogenases and they all require more than ten Fe atoms per functional protein complex (Khetkorn et al., 2013). All heterologously expressed hydrogenases could therefore interfere with the iron need of photosynthesis and other Fe-rich enzymes such as nitrogenase (Shi et al., 2007). However, long term iron depletion (~90 days) in *Nostoc* PCC 7120 wildtype has shown that the mechanism of iron homeostasis is highly regulated ensuring the activity of photosynthesis and nitrogen fixation at a lower but stable level already after some days of cultivation (Narayan et al., 2011). Due to the high turnover number of hydrogenases (Nagarajan et al., 2017), a well-regulated expression level that matches the metabolic capacity for H_2 production should be the major objective, minimizing the hydrogenase's metabolic burden on the available intracellular iron. Furthermore, a reliable hydrogenase activation process on the transcription level could be implemented to time its expression with the onset of iron limitation effects. Simultaneously, as the level of nitrogenase activity naturally declines upon iron starvation (Narayan et al., 2011), the residual iron utilized for nitrogen fixation could be reallocated to the [FeFe] hydrogenase complex. Nevertheless, a basal level of nitrogen fixation will be needed for the stabilization of the culture ensuring proteome maintenance e.g. the repair mechanism of photosystem II (Latifi et al., 2009). Thus, Fe-limited cultures could serve as a heterocyst-based production platform for H_2, while the nitrogenase activity remains low. As Fe limitation effectively reduces cyanobacterial growth and enhances the accumulation of carbohydrates inside the cells, it is a promising cultivation strategy to harness the photosynthetically stored energy for H_2 biosynthesis. Instead of allowing continuous growth of cyanobacteria in photobioreactors, which has been the promoted

strategy in the past 30 years of biofuel research (Luan et al., 2019), the sunlight energy needs to directly find its way into H₂ or other fuels, not via biomass.

4. Conclusions

In this study we show that a Fe-limited cultivation strategy supports major cellular properties that are essential for a photobiological H₂ production platform. For efficient H₂ production a photo-fermentative pathway needs to be introduced to *Nostoc* PCC 7120 Δ*hupW*. For this, we propose a well-regulated heterologous expression of a H₂-producing hydrogenase in the heterocysts of *Nostoc*.

CRediT authorship contribution statement

Christoph Howe: Conceptualization, Investigation, Methodology, Writing - original draft, Formal analysis, Visualization.**Daniel Becker:** Investigation.**Christian Steinweg:**Methodology, Investigation. **Clemens Posten:**Supervision, Resources.**Karin Stensjö:**Supervision, Writing - review & editing.

Declaration of competing interest

The authors declare that they have no known competing financial interests or personal relationships that could have appeared to influence the work reported in this paper.

Appendix A. Supplementary data

Supplementary data to this article can be found online at https://doi.org/10.1016/j.biteb.2020.100508.

References

Ananyev, G., Carrieri, D., Dismukes, G.C., 2008. Optimization of metabolic capacity and flux through environmental cues to maximize hydrogen production by the cyanobacterium "*Arthrospira* (*Spirulina*) *maxima*". Appl. Environ. Microbiol. 74, 6102–6113.
Avilan, L., Roumezi, B., Risoul, V., Bernard, C.S., Kpebe, A., Belhadjhassine, M., Rousset, M., Brugna, M., Latifi, A., 2018. Phototrophic hydrogen production from a clostridial [FeFe] hydrogenase expressed in the heterocysts of the cyanobacterium *Nostoc* PCC 7120. Appl. Microbiol. Biotechnol. 102, 5775–5783.
Berberoğlu, H., Jay, J., Pilon, L., 2008. Effect of nutrient media on photobiological hydrogen production by *Anabaena variabilis* ATCC 29413. Int. J. Hydrog. Energy 33, 1172–1184.
Borodin, V.B., Tsygankov, A.A., Rao, K.K., Hall, D.O., 2000. Hydrogen production by *Anabaena variabilis* PK84 under simulated outdoor conditions. Biotechnol. Bioeng. 69, 478–485.
Boyd, P.W., Jickells, T., Blain, S., Follows, M., Owens, N.P.J., de Baar, H.J.W., Boyle, E.A., Coale, K.H., Schoemann, V., Levasseur, M., Pollard, R., Rivkin, R.B., Takeda, S., Harvey, M., Lancelot, C., Sarmiento, J., Smetacek, V., Tsuda, A., Buesseler, K.O., Law, C.S., Cullen, J.J., Turner, S., Watson, A.J., 2007. Mesoscale iron enrichment experiments 1993–2005: synthesis and future directions. Science 315, 612–617.
Brausam, A., Maigut, J., Meier, R., Szilágyi, P.Á., Buschmann, H.J., Massa, W., Homonnay, Z., Van Eldik, R., 2009. Detailed spectroscopic, thermodynamic, and

kinetic studies on the protolytic equilibria of FeIIIcydta and the activation of hydrogen peroxide. Inorg. Chem. 48, 7864–7884.
Dougals, D., Peat, A., Whitton, B.A., Wood, P., 1986. Influence of iron status on structure of the cyanobacterium (blue-green alga) *Calothrix parietina*. Cytobios 47, 155–166.
Hardie, L.P., Balkwill, D.L., Stevens, S.E., 1983. Effects of iron starvation on the ultrastructure of the cyanobacterium *Agmenellum quadruplicatum*. Appl. Environ. Microbiol. 45, 1007–1017.
Jacq, V., Ridame, C., L'Helguen, S., Kaczmar, F., Saliot, A., 2014. Response of the unicellular diazotrophic cyanobacterium *Crocosphaera watsonii* to iron limitation. PLoS One 9, 1–9.
Kars, G., Gündüz, U., 2010. Towards a super H₂ producer: improvements in photofermentative biohydrogen production by genetic manipulations. Int. J. Hydrogen Energy 35, 6646–6656.
Khetkorn, W., Khanna, N., Incharoensakdi, A., Lindblad, P., 2013. Metabolic and genetic engineering of cyanobacteria for enhanced hydrogen production. Biofuels 4, 535–561.
Kranzler, C., Rudolf, M., Keren, N., Schleiff, E., 2013. Iron in cyanobacteria. Adv. Bot. Res. 65, 57–105.
Latifi, A., Ruiz, M., Zhang, C.C., 2009. Oxidative stress in cyanobacteria. FEMS Microbiol. Rev. 33, 258–278.
Liberton, M., Collins, A.M., Page, L.E., O'Dell, W.B., O'Neill, H., Urban, V.S., Timlin, J.A., Pakrasi, H.B., 2013. Probing the consequences of antenna modification in cyanobacteria. Photosynth. Res. 118, 17–24.
Lindberg, P., Devine, E., Stensjö, K., Lindblad, P., 2012. HupW protease specifically required for processing of the catalytic subunit of the uptake hydrogenase in the cyanobacterium *Nostoc* sp. strain PCC 7120. Appl. Environ. Microbiol. 78, 273–276.
Lindblad, P., Christensson, K., Lindberg, P., Fedorov, A., Pinto, F., Tsygankov, A., 2002. Photoproduction of H₂ by wildtype *Anabaena* PCC 7120 and a hydrogen uptake deficient mutant: from laboratory experiments to outdoor culture. Int. J. Hydrogen Energy 27, 1271–1281.
Luan, G., Zhang, S., Wang, M., Lu, X., 2019. Progress and perspective on cyanobacterial glycogen metabolism engineering. Biotechnol. Adv. 37, 771–786.
Magnuson, A., 2019. Heterocyst thylakoid bioenergetics. Life 9, 1–13.
Masukawa, H., Mochimaru, M., Sakurai, H., 2002. Disruption of the uptake hydrogenase gene, but not of the bidirectional hydrogenase gene, leads to enhanced photobiological hydrogen production by the nitrogen-fixing cyanobacterium *Anabaena* sp. PCC 7120. Appl. Microbiol. Biotechnol. 58, 618–624.
Masukawa, H., Inoue, K., Sakurai, H., Wolk, C.P., Hausinger, R.P., 2010. Site-directed mutagenesis of the *Anabaena* sp. strain PCC 7120 nitrogenase active site to increase photobiological hydrogen production. Appl. Environ. Microbiol. 76, 6741–6750.
Masukawa, H., Sakurai, H., Hausinger, R.P., Inoue, K., 2017. Increased heterocyst frequency by patN disruption in *Anabaena* leads to enhanced photobiological hydrogen production at high light intensity and high cell density. Appl. Microbiol. Biotechnol. 101, 2177–2188.
Melis, A., Zhang, L., Forestier, M., Ghirardi, M.L., Seibert, M., 2000. Sustained photobiological hydrogen gas production upon reversible inactivation of oxygen evolution in the green alga *Chlamydomonas reinhardtii*. Plant Physiol. 122, 127–136.
Nagarajan, D., Lee, D.J., Kondo, A., Chang, J.S., 2017. Recent insights into biohydrogen production by microalgae – from biophotolysis to dark fermentation. Bioresour. Technol. 227, 373–387.
Narayan, Prakash, O., Kumari, N., Rai, L.C., 2011. Iron starvation-induced proteomic changes in *Anabaena* (*Nostoc*) sp. PCC 7120: exploring survival strategy. J. Microbiol. Biotechnol. 21, 136–146.
Nyberg, M., Heidorn, T., Lindblad, P., 2015. Hydrogen production by the engineered cyanobacterial strain *Nostoc* PCC 7120 ΔhupW examined in a flat panel photobioreactor system. J. Biotechnol. 215, 35–43.
Prince, R.C., Kheshgi, H.S., 2005. The photobiological production of hydrogen: potential efficiency and effectiveness as a renewable fuel. Crit. Rev. Microbiol. 31, 19–31.
Quigg, A., 2016. Micronutrients. In: Borowitzka, M.A., Beardall, J., Raven, J.A. (Eds.), Physiology of microalgae. Springer, Switzerland, pp. 211–231.
Rippka, R., Deruelles, J., Waterbury, J.B., Herdman, M., Stanier, R.Y., 1979. Generic assignments, strain histories and properties of pure cultures of cyanobacteria. Microbiology 111, 1–61.
Rodionova, M.V., Poudyal, R.S., Tiwari, I., Voloshin, R.A., Zharmukhamedov, S.K., Nam, H.G., Zayadan, B.K., Bruce, B.D., Hou, H.J.M., Allakhverdiev, S.I., 2017. Biofuel production: challenges and opportunities. Int. J. Hydrogen Energy 42, 8450–8461.
Saifuddin, N., Priatharsini, P., 2016. Developments in bio-hydrogen production from algae: a review. Res. J. Appl. Sci. Eng. Technol. 12, 968–982.
Sakurai, H., Masukawa, H., Kitashima, M., Inoue, K., 2015. How close we are to achieving commercially viable large-scale photobiological hydrogen production by cyanobacteria: a review of the biological aspects. Life 5, 997–1018.
Salleh, S.F., Kamaruddin, A., Uzir, M.H., Karim, K.A., Mohamed, A.R., 2016. Investigation of the links between heterocyst and biohydrogen production by diazotrophic cyanobacterium *A. variabilis* ATCC 29413. Arch. Microbiol. 198, 101–113.
Schoffman, H., Keren, N., 2019. Function of the IsiA pigment–protein complex in vivo. Photosynth. Res. 141, 343–353.
Sherman, D.M., Sherman, L.A., 1983. Effect of iron deficiency and iron restoration on ultrastructure of *Anacystis nidulans*. J. Bacteriol. 156, 393–401.
Shi, T., Sun, Y., Falkowski, P.G., 2007. Effects of iron limitation on the expression of metabolic genes in the marine cyanobacterium *Trichodesmium erythraeum* IMS101. Environ. Microbiol. 9, 2945–2956.
Staal, M., te Lintel-Hekkert, S., Harren, F., Stal, L., 2001. Nitrogenase activity in cyanobacteria measured by the acetylene reduction assay: a comparison between batch incubation and on-line monitoring. Environ. Microbiol. 3, 343–351.
Straus, N.A., 1994. Iron deprivation: physiology and gene regulation. The molecular biology of cyanobacteria. Advances in Photosynthesis. Bryant, D.A. (Ed.), 1.

Springer, Dordrecht, pp. 731–750.

van Alphen, P., Abedini Najafabadi, H., Branco dos Santos, F., Hellingwerf, K.J., 2018. Increasing the photoautotrophic growth rate of *Synechocystis* sp. PCC 6803 by identifying the limitations of its cultivation. Biotechnol. J. 13, 1–8.

Yeager, C.M., Milliken, C.E., Bagwell, C.E., Staples, L., Berseth, P.A., Sessions, H.T., 2011. Evaluation of experimental conditions that influence hydrogen production among heterocystous cyanobacteria. Int. J. Hydrog. Energy 36, 7487–7499.

Yemm, E.W., Willis, A.J., 1954. The estimation of carbohydrates in plant extracts by anthrone. Biochem. J. 57, 508–514.

Yingping, F., Lemeille, S., Talla, E., Janicki, A., Denis, Y., Zhang, C.C., Latifi, A., 2014. Unravelling the cross-talk between iron starvation and oxidative stress responses highlights the key role of PerR (alr0957) in peroxide signalling in the cyanobacterium *Nostoc* PCC 7120. Environ. Microbiol. Rep. 6, 468–475.

Zavřel, T., Sinetova, M., Červený, J., 2015. Measurement of chlorophyll a and carotenoids concentration in cyanobacteria. Bio-Protocol 5. https://doi.org/10.21769/BioProtoc.1467.